

## Nonlinear stochastic optimal control strategy of hysteretic structures

Jie Li<sup>1,3a</sup>, Yong-Bo Peng<sup>\*2,3</sup> and Jian-Bing Chen<sup>1,3b</sup>

<sup>1</sup>School of Civil Engineering, Tongji University, 1239 Siping Road, Shanghai 200092, P.R. China

<sup>2</sup>Shanghai Insititute of Disaster Prevention and Relief, Tongji University, 1239 Siping Road, Shanghai 200092, P.R. China

<sup>3</sup>State Key Laboratory of Disaster Reduction in Civil Engineering, Tongji University, 1239 Siping Road, Shanghai, 200092, P.R. China

(Received September 26, 2009, Accepted November 24, 2010)

**Abstract.** Referring to the formulation of physical stochastic optimal control of structures and the scheme of optimal polynomial control, a nonlinear stochastic optimal control strategy is developed for a class of structural systems with hysteretic behaviors in the present paper. This control strategy provides an amenable approach to the classical stochastic optimal control strategies, bypasses the dilemma involved in Itô-type stochastic differential equations and is applicable to the dynamical systems driven by practical non-stationary and non-white random excitations, such as earthquake ground motions, strong winds and sea waves. The newly developed generalized optimal control policy is integrated in the nonlinear stochastic optimal control scheme so as to logically distribute the controllers and design their parameters associated with control gains. For illustrative purposes, the stochastic optimal controls of two base-excited multi-degree-of-freedom structural systems with hysteretic behavior in Clough bilinear model and Bouc-Wen differential model, respectively, are investigated. Numerical results reveal that a linear control with the 1st-order controller suffices even for the hysteretic structural systems when a control criterion in exceedance probability performance function for designing the weighting matrices is employed. This is practically meaningful due to the nonlinear controllers which may be associated with dynamical instabilities being saved. It is also noted that using the generalized optimal control policy, the maximum control effectiveness with the few number of control devices can be achieved, allowing for a desirable structural performance. It is remarked, meanwhile, that the response process and energy-dissipation behavior of the hysteretic structures are controlled to a certain extent.

**Keywords:** physical stochastic optimal control; polynomial controllers; exceedance probability; generalized optimal control policy; hysteretic structures; structural performance.

---

### 1. Introduction

The response of structural systems usually excurses inelastic range back and forth when subjected to severe environmental loads associated with earthquakes, strong winds and recurrent waves. It is

---

\*Corresponding author, Ph.D., E-mail: pengyongbo@tongji.edu.cn

<sup>a</sup>Distinguished Professor, E-mail: lijie@tongji.edu.cn

<sup>b</sup>Associate Professor, E-mail: chenjb@tongji.edu.cn

the so-called hysteretic behavior of structures where the restoring force of structural components depends not only on the present structural displacement, also on the previous structural states. Many mathematical models have been developed to efficiently describe the hysteretic behavior of structures in random vibration analysis. Two classes of them are widely used in structural engineering and materials, i.e. the bilinear elasto-plastic model (Iwan 1961, Clough and Johnson 1966) and the Bouc-Wen differential model (Bouc 1967, Wen 1976, Baber and Wen 1981, Baber and Noori 1985). They are often employed to describe the characteristics of reinforced concrete, steel, base isolators and dampers, etc. As a counterpart approach to structural performance design, the nonlinear optimal control strategy has been paid increasing attentions since the concept of structural control was proposed in the early of 1970s (Yao 1972). For example, in 1981 Masri *et al.* presented an optimum pulse control method for reducing the oscillations of nonlinear flexible systems in response to arbitrary dynamic environments (Masri *et al.* 1981). Yang *et al.* (1988) developed the instantaneous optimal control algorithms for applications to control of nonlinear and hysteretic structures and extended the method to aseismic hybrid control systems (Yang *et al.* 1988, 1992). Suhardjo *et al.* (1992) developed a class of optimal polynomial control methods based on series expansions of the optimal cost function and the optimal control function in a Hamilton-Jacobi context (Suhardjo *et al.* 1992).

However, the probabilistic treatment of nonlinear optimal control of structures did not receive enough attention. Actually, the stochastic optimal control strategies in the present literatures are exclusively hinged on Itô-type stochastic differential equations, of which the random disturbance term specifying external excitations and measurement noises is mathematically assumed to be independent additive Gaussian white noise or filtered Gaussian white noise. For instance, Shefer and Breakwell developed an optimal digital nonlinear feedback control law for specified nonlinear systems by taking into account the non-Gaussian character of the state conditional distribution. They involved 1st-order moment and higher-order moments of the conditional distribution in the state estimate (Shefer and Breakwell 1987). Yang *et al.* studied a stochastic hybrid control procedure of seismic-excited base-isolated buildings using the methods of random vibration and equivalent linearization, where the earthquake ground motion is modeled as a filtered shot noise (Yang *et al.* 1994). Zhu *et al.* proposed a nonlinear stochastic optimal control strategy of hysteretic systems under random excitations based on the stochastic averaging method and stochastic dynamical programming principle. An averaged Itô equation for the total energy of the system was defined as a one-dimensional controlled diffusion process (Zhu *et al.* 2000).

It is noted that the classical stochastic optimal control strategies are still open to the practical non-stationary, non-Gaussian stochastic process driven systems. Recently, a physical approach to structural stochastic optimal controls on the basis of the generalized density evolution equation has been proposed by the authors, which is applicable to practical random excitation driven linear systems (Li *et al.* 2010a). We thus attempt to develop a nonlinear stochastic optimal control strategy of a hysteretic structures based on the optimal polynomial control scheme. The newly developed generalized optimal control policy is employed whereby the design parameters and placements of few number of control devices are laid down so as to make the control effectiveness maximized. For illustrative purposes, the stochastic optimal controls of two base-excited multi-degree-of-freedom structural systems with hysteretic behavior in Clough bilinear model and Bouc-Wen differential model, respectively, are carried out as the numerical examples.

The sections arranged in this paper are distributed as follows. Section 2 is devoted to to developing a stochastic optimal polynomial control strategy adapted to nonlinear stochastic

dynamical systems according to the optimal polynomial control scheme. Section 3 illustrates the probability density evolution of the state and control force vectors of controlled systems, which is governed by generalized density evolution equations. The design of controllers is preceded in Section 4, which is based on the control gain criterion and control topology criterion in exceedance probability. The control policy deduced from the control criteria is referred to be the generalized optimal control policy, which includes the optimal parameters and the optimal placements of controllers. Case studies are carried out in Section 5. Two base-excited multi-degree-of-freedom hysteretic structures with behavior in Clough bilinear model and Bouc-Wen differential model are investigated as numerical examples, respectively. The concluding remarks are included in the final section.

## 2. Optimal polynomial control of nonlinear stochastic dynamical systems

Without loss of generality, an  $n$ -degree-of-freedom nonlinear system subjected to a finite mean-square random excitation  $\mathbf{F}(\varpi, t)$  is investigated. The vector equation of motion is given by

$$\mathbf{M}\ddot{\mathbf{X}}(t) + \mathbf{f}[\mathbf{X}(t), \dot{\mathbf{X}}(t)] = \mathbf{B}_s \mathbf{U}(t) + \mathbf{D}_s \mathbf{F}(\varpi, t), \quad \mathbf{X}(t_0) = \mathbf{x}_0; \quad \dot{\mathbf{X}}(t_0) = \dot{\mathbf{x}}_0 \quad (1)$$

where  $\mathbf{X}(t) = \mathbf{X}(\Theta, t)$  is an  $n$ -dimensional displacement vector;  $\mathbf{U}(t) = \mathbf{U}(\Theta, t)$  is an  $r$ -dimensional control force vector;  $\mathbf{F}(\cdot)$  is a  $p$ -dimensional random excitation vector, in which  $\varpi$  represent a point in the probability space, i.e. an embedded basic random event characterizing the randomness in the external excitation.  $\Theta = \Theta(\varpi)$  denotes a random parameter vector mapped from  $\varpi$  which implicitly underlies the state and control force vectors, and has the joint PDF  $p_\Theta(\theta)$ .  $\mathbf{M}$  is an  $n \times n$  mass matrix;  $\mathbf{f}[\cdot]$  is an  $n$ -dimensional nonlinear internal force vector;  $\mathbf{B}_s$  is an  $n \times r$  matrix denoting the location of controllers;  $\mathbf{D}_s$  is an  $n \times p$  matrix denoting the location of excitations.

It should be noted that the randomness denoted by  $\Theta$  is typically considered to be resulting from the external excitation in this paper, and the measurement noise usually taken into account in the classical stochastic optimal controls is neglected since the uncertainty arising from the measurement noise is more controllable compared with that of the random excitation. Meanwhile, it is felt that, although somewhat cumbersome, the notation  $\Theta$  underlies the fact that a random process is a function defined over the space of events of which  $\Theta$  is an element. Having noted this, the symbol  $\Theta$  would be dropped in the following development when the random nature of a certain quantity is obvious from the context except in the case of special denotation for a key quantity.

The physical stochastic optimal control strategy developed by Li *et al.*, as was mentioned previously, involves solving a number of deterministic dynamic evolution equations evaluated at the representative points in sample space with pre-assigned-weights (Li *et al.* 2010a). Hence, it is natural to develop the stochastic optimal polynomial control strategy by incorporating the formulation of physical stochastic optimal control and the deterministic nonlinear control theory. The optimal polynomial control, as a preferred nonlinear optimal control strategy, will be employed in the following development. This control strategy involves two step optimizations. In the first step, for each representative realization  $\theta$  of stochastic parameters  $\Theta$ , the minimization of a cost function is carried out to build up a functional mapping from the set of parameters of control policy to the set of control gains. In the second step, the specified parameters of control policy and the corresponding control gain are obtained by minimizing a performance function related to the objective structural performance.

Optimal polynomial control was proposed according to Hamilton-Jacobi theoretical framework and the optimal principle (Suhardjo *et al.* 1992). It is essentially the extended formulation of the linear quadratic regulator (LQR) control in state space. In order to write the Eq. (1) as the form of its state equation with separation between system matrix and state vector, the nonlinear internal force  $\mathbf{f}[\cdot]$  needs to be expanded. It can be expressed as the following Maclaurin series

$$\begin{aligned} \mathbf{f}[\mathbf{X}(t), \dot{\mathbf{X}}(t)] = & \mathbf{f}[\mathbf{0}, \mathbf{0}] + \left( \mathbf{X} \frac{\partial \mathbf{f}[\mathbf{X}, \dot{\mathbf{X}}]}{\partial \mathbf{X}} + \dot{\mathbf{X}} \frac{\partial \mathbf{f}[\mathbf{X}, \dot{\mathbf{X}}]}{\partial \dot{\mathbf{X}}} \right) \Bigg|_{\mathbf{X}=\mathbf{0}, \dot{\mathbf{X}}=\mathbf{0}} \\ & + \frac{1}{2!} \left( \mathbf{X}^2 \frac{\partial^2 \mathbf{f}[\mathbf{X}, \dot{\mathbf{X}}]}{\partial \mathbf{X}^2} + \mathbf{X} \dot{\mathbf{X}} \frac{\partial^2 \mathbf{f}[\mathbf{X}, \dot{\mathbf{X}}]}{\partial \mathbf{X} \partial \dot{\mathbf{X}}} + \dot{\mathbf{X}}^2 \frac{\partial^2 \mathbf{f}[\mathbf{X}, \dot{\mathbf{X}}]}{\partial \dot{\mathbf{X}}^2} \right) \Bigg|_{\mathbf{X}=\mathbf{0}, \dot{\mathbf{X}}=\mathbf{0}} \\ & + \dots + \frac{1}{m!} \left( \mathbf{X}^m \frac{\partial^m \mathbf{f}[\mathbf{X}, \dot{\mathbf{X}}]}{\partial \mathbf{X}^m} + \sum_{k=1}^{m-1} \mathbf{X}^{m-k} \dot{\mathbf{X}}^k \frac{\partial^m \mathbf{f}[\mathbf{X}, \dot{\mathbf{X}}]}{\partial \mathbf{X}^{m-k} \partial \dot{\mathbf{X}}^k} + \dot{\mathbf{X}}^m \frac{\partial^m \mathbf{f}[\mathbf{X}, \dot{\mathbf{X}}]}{\partial \dot{\mathbf{X}}^m} \right) \Bigg|_{\mathbf{X}=\mathbf{0}, \dot{\mathbf{X}}=\mathbf{0}} \end{aligned} \quad (2)$$

It is noted that for most nonlinear systems, the terms including the cross-product between  $\mathbf{X}^i$  and  $\dot{\mathbf{X}}^i$  might not affect the nonlinear internal force, or their contribution is far less than that of other terms. The cross-product terms in Eq. (2) could thus be dropped in the following development. Moreover, the nonlinear internal force is typically zero when the state vector is zero. We thus have

$$\begin{aligned} \mathbf{f}[\mathbf{X}(t), \dot{\mathbf{X}}(t)] = & \mathbf{X} \left( \frac{\partial \mathbf{f}[\mathbf{X}, \dot{\mathbf{X}}]}{\partial \mathbf{X}} + \frac{1}{2!} \mathbf{X} \frac{\partial^2 \mathbf{f}[\mathbf{X}, \dot{\mathbf{X}}]}{\partial \mathbf{X}^2} + \dots + \frac{1}{m!} \mathbf{X}^{m-1} \frac{\partial^m \mathbf{f}[\mathbf{X}, \dot{\mathbf{X}}]}{\partial \mathbf{X}^m} \right) \Bigg|_{\mathbf{X}=\mathbf{0}, \dot{\mathbf{X}}=\mathbf{0}} \\ & + \dot{\mathbf{X}} \left( \frac{\partial \mathbf{f}[\mathbf{X}, \dot{\mathbf{X}}]}{\partial \dot{\mathbf{X}}} + \frac{1}{2!} \dot{\mathbf{X}} \frac{\partial^2 \mathbf{f}[\mathbf{X}, \dot{\mathbf{X}}]}{\partial \dot{\mathbf{X}}^2} + \dots + \frac{1}{m!} \dot{\mathbf{X}}^{m-1} \frac{\partial^m \mathbf{f}[\mathbf{X}, \dot{\mathbf{X}}]}{\partial \dot{\mathbf{X}}^m} \right) \Bigg|_{\mathbf{X}=\mathbf{0}, \dot{\mathbf{X}}=\mathbf{0}} \end{aligned} \quad (3)$$

In the state space, Eq. (1) can be written in the form

$$\dot{\mathbf{Z}}(t) = \Lambda(\mathbf{Z})\mathbf{Z}(t) + \mathbf{B}\mathbf{U}(t) + \mathbf{D}\mathbf{F}(\varpi, t) \quad (4)$$

with the initial condition  $\mathbf{Z}(t_0) = \mathbf{z}_0$ , where  $\mathbf{Z}(t)$  is a  $2n$ -dimensional state vector;  $\Lambda(\mathbf{Z})$  is a  $2n \times 2n$  system matrix;  $\mathbf{B}$  is a  $2n \times r$  controllers location matrix, and  $\mathbf{D}$  is a  $2n \times p$  excitation location matrix, respectively

$$\begin{aligned} \mathbf{Z}(t) = & \begin{bmatrix} \mathbf{X}(t) \\ \dot{\mathbf{X}}(t) \end{bmatrix}, \mathbf{B} = \begin{bmatrix} \mathbf{0} \\ \mathbf{M}^{-1}\mathbf{B}_s \end{bmatrix}, \mathbf{D} = \begin{bmatrix} \mathbf{0} \\ \mathbf{M}^{-1}\mathbf{D}_s \end{bmatrix} \\ \Lambda(\mathbf{Z}) = & \begin{bmatrix} \mathbf{0} & \mathbf{I} \\ -\mathbf{M}^{-1} \sum_{i=0}^m \frac{\mathbf{X}^{i-1}}{i!} \frac{\partial^i \mathbf{f}[\mathbf{X}(t), \dot{\mathbf{X}}(t)]}{\partial \mathbf{X}^i} \Bigg|_{\mathbf{X}=\mathbf{0}, \dot{\mathbf{X}}=\mathbf{0}} & -\mathbf{M}^{-1} \sum_{i=0}^m \frac{\dot{\mathbf{X}}^{i-1}}{i!} \frac{\partial^i \mathbf{f}[\mathbf{X}(t), \dot{\mathbf{X}}(t)]}{\partial \dot{\mathbf{X}}^i} \Bigg|_{\mathbf{X}=\mathbf{0}, \dot{\mathbf{X}}=\mathbf{0}} \end{bmatrix} \end{aligned} \quad (5)$$

where  $m$  is the highest order of the Maclaurin's series, and is equal to the highest order of the nonlinear internal force, indicating that the terms of series with  $(m + 1)$  order and higher orders are all zeros.

A polynomial cost function, in stochastic scenario with  $\Theta$ , is given by (Yang *et al.* 1996)

$$J_1(\mathbf{Z}, \mathbf{U}, \Theta, t) = \mathbf{S}(\mathbf{Z}(t_f), t_f) + \frac{1}{2} \int_{t_0}^{t_f} [\mathbf{Z}^T(t) \mathbf{Q}_Z \mathbf{Z}(t) + \mathbf{U}^T(t) \mathbf{R}_U \mathbf{U}(t) + \mathbf{h}(\mathbf{Z}, t)] dt \quad (6)$$

where  $\mathbf{S}(\mathbf{Z}(t_f), t_f)$  is the terminal cost;  $t_0, t_f$  are the start and terminal time, respectively;  $\mathbf{Q}_Z$  is a  $2n \times 2n$  positive semi-definite state weighting matrix;  $\mathbf{R}_U$  is an  $r \times r$  positive-definite control weighting matrix;  $\mathbf{h}(\mathbf{Z}, t)$  is the higher-order term of the cost function whose orders are higher than the quadratic term. It is indicated that the terminal cost, together with the first two terms of the integrand in Eq. (6) conduct the canonical LQR control.

For a given realization  $\theta$  of stochastic parameter vector  $\Theta$ , as indicated in the physical scheme of structural stochastic optimal control (Li *et al.* 2010a), the minimization of the polynomial cost function Eq. (6) will result in the celebrated Hamilton-Jacobi-Bellman equation (Anderson and Moore 1990)

$$\frac{\partial V(\mathbf{Z}, t)}{\partial t} = -\min_{\mathbf{U}} [H(\mathbf{Z}, \mathbf{U}, V'(\mathbf{Z}, t), \Theta, t)] \quad (7)$$

where a prime indicates the differentiation with respect to  $\mathbf{Z}$ ;  $V(\mathbf{Z}, t)$  is the optimal cost function, and satisfies all the properties of a Lyapunov function (Bernstein 1993), considered as

$$V(\mathbf{Z}, t) = \frac{1}{2} \mathbf{Z}^T(t) \mathbf{P}(t) \mathbf{Z}(t) + g(\mathbf{Z}, t) \quad (8)$$

where  $\mathbf{P}(t)$  is a  $2n \times 2n$  Riccati matrix, which will be defined in the following Eq. (15);  $g(\mathbf{Z}, t)$  is a positive definite multinomial in  $\mathbf{Z}(t)$ .

The necessary condition for the minimization of the right-hand side of Eq. (7) is

$$\frac{\partial H(\mathbf{Z}, \mathbf{U}, V'(\mathbf{Z}, t), \Theta, t)}{\partial \mathbf{U}} = \mathbf{0} \quad (9)$$

Since the probabilistic criterion used in the physical stochastic optimal control of structures relies on the structural response performance, which actually includes the effect of the external excitation integrated over all its possible realizations (Li *et al.* 2010b). Therefore, the excitation-relevant term in the feedback gain expression can be safely dropped, resulting in a closed-loop control with the state-feedback. The extended Hamiltonian function  $\mathbf{H}(\cdot)$  is given by

$$\begin{aligned} H(\mathbf{Z}, \mathbf{U}, V'(\mathbf{Z}, t), \Theta, t) &= \frac{1}{2} [\mathbf{Z}^T(t) \mathbf{Q}_Z \mathbf{Z}(t) + \mathbf{U}^T(t) \mathbf{R}_U \mathbf{U}(t) + \mathbf{h}(\mathbf{Z}, t)] \\ &\quad + [V'(\mathbf{Z}, t)]^T (\mathbf{A}(\mathbf{Z}) \mathbf{Z}(t) + \mathbf{B} \mathbf{U}(t)) \end{aligned} \quad (10)$$

Having Eq. (8) in mind, we have

$$\begin{aligned} H(\mathbf{Z}, \mathbf{U}, V'(\mathbf{Z}, t), \Theta, t) &= \frac{1}{2} [\mathbf{Z}^T(t) \mathbf{Q}_Z \mathbf{Z}(t) + \mathbf{U}^T(t) \mathbf{R}_U \mathbf{U}(t) + \mathbf{h}(\mathbf{Z}, t)] \\ &\quad + [\mathbf{Z}^T(t) \mathbf{P}(t) + (g'(\mathbf{Z}, t))^T] (\mathbf{A}(\mathbf{Z}) \mathbf{Z}(t) + \mathbf{B} \mathbf{U}(t)) \end{aligned} \quad (11)$$

Substitution of Eq. (11) into the necessary condition in Eq. (9) leads to

$$\mathbf{R}_U \mathbf{U}(t) + \mathbf{B}^T \mathbf{P}(t) \mathbf{Z}(t) + \mathbf{B}^T g'(\mathbf{Z}, t) = \mathbf{0} \quad (12)$$

The optimal non-linear controller is then given as follows

$$\mathbf{U}(t) = -\mathbf{R}_U^{-1} \mathbf{B}^T \mathbf{P}(t) \mathbf{Z}(t) - \mathbf{R}_U^{-1} \mathbf{B}^T g'(\mathbf{Z}, t) \quad (13)$$

It is also clear from Eq. (12) that

$$\frac{\partial^2 H(\mathbf{Z}, \mathbf{U}, V'(\mathbf{Z}, t), \Theta, t)}{\partial \mathbf{U}^2} = \mathbf{R}_U > \mathbf{0} \quad (14)$$

Therefore, the minimum control definitely exists.

Substituting Eqs. (8), (11) and (13) into Eq. (7), and separating quadratic terms in  $\mathbf{Z}(t)$  from terms containing  $g(\mathbf{Z}, t)$ , one obtains

$$-\dot{\mathbf{P}}(t) = \mathbf{P}(t)\Lambda(\mathbf{Z}) + \Lambda^T(\mathbf{Z})\mathbf{P}(t) - \mathbf{P}(t)\mathbf{B}\mathbf{R}_U^{-1}\mathbf{B}^T\mathbf{P}(t) + \mathbf{Q}_Z \quad (15)$$

$$-\dot{g}(\mathbf{Z}, t) = \frac{1}{2}h(\mathbf{Z}, t) - \frac{1}{2}(g'(\mathbf{Z}, t))^T \mathbf{B}\mathbf{R}_U^{-1}\mathbf{B}^T g'(\mathbf{Z}, t) + (g'(\mathbf{Z}, t))^T [\Lambda(\mathbf{Z}) - \mathbf{B}\mathbf{R}_U^{-1}\mathbf{B}^T\mathbf{P}(t)]\mathbf{Z}(t) \quad (16)$$

The scalar identity

$$2\mathbf{P}(t)\Lambda(\mathbf{Z}) = \mathbf{P}(t)\Lambda(\mathbf{Z}) + \Lambda^T(\mathbf{Z})\mathbf{P}(t) \quad (17)$$

has been used in Eq. (15). To express the controller in Eq. (13) as an explicit function,  $g(\mathbf{Z}, t)$  is chosen in the following form (Yang *et al.* 1996)

$$g(\mathbf{Z}, t) = \sum_{i=2}^k \frac{1}{i} [\mathbf{Z}^T(t)\mathbf{M}_i(t)\mathbf{Z}(t)]^i \quad (18)$$

where  $\mathbf{M}_i(t)$ ,  $i = 2, 3, \dots, k$  are  $2n \times 2n$  Lyapunov matrices to be defined in the following Eq. (21).

Substituting Eq. (18) into Eq. (16), we then have

$$\begin{aligned} & -2 \sum_{i=2}^k [\mathbf{Z}^T(t)\mathbf{M}_i(t)\mathbf{Z}(t)]^{i-1} \mathbf{Z}^T(t)\dot{\mathbf{M}}_i(t)\mathbf{Z}(t) = \mathbf{h}(\mathbf{Z}, t) \\ & -4 \left\{ \sum_{i=2}^k [\mathbf{Z}^T(t)\mathbf{M}_i(t)\mathbf{Z}(t)]^{i-1} \mathbf{M}_i(t)\mathbf{Z}(t) \right\}^T \mathbf{B}\mathbf{R}_U^{-1}\mathbf{B}^T \left\{ \sum_{i=2}^k [\mathbf{Z}^T(t)\mathbf{M}_i(t)\mathbf{Z}(t)]^{i-1} \mathbf{M}_i(t)\mathbf{Z}(t) \right\} \\ & + 4 \left\{ \sum_{i=2}^k [\mathbf{Z}^T(t)\mathbf{M}_i(t)\mathbf{Z}(t)]^{i-1} \mathbf{M}_i(t)\mathbf{Z}(t) \right\}^T [\Lambda(\mathbf{Z}) - \mathbf{B}\mathbf{R}_U^{-1}\mathbf{B}^T\mathbf{P}(t)]\mathbf{Z}(t) \end{aligned} \quad (19)$$

Let

$$\begin{aligned} \mathbf{h}(\mathbf{Z}, t) &= 2 \left\{ \sum_{i=2}^k [\mathbf{Z}^T(t)\mathbf{M}_i(t)\mathbf{Z}(t)]^{i-1} \mathbf{Z}(t) \right\}^T \mathbf{Q}_{Z,i}(t)\mathbf{Z}(t) + \\ & 4 \left\{ \sum_{i=2}^k [\mathbf{Z}^T(t)\mathbf{M}_i(t)\mathbf{Z}(t)]^{i-1} \mathbf{M}_i(t)\mathbf{Z}(t) \right\}^T \mathbf{B}\mathbf{R}_U^{-1}\mathbf{B}^T \left\{ \sum_{i=2}^k [\mathbf{Z}^T(t)\mathbf{M}_i(t)\mathbf{Z}(t)]^{i-1} \mathbf{M}_i(t)\mathbf{Z}(t) \right\} \end{aligned} \quad (20)$$

such that simple analytical solution can be obtained, where  $\mathbf{Q}_{Z,i}$ ,  $i = 2, 3, \dots, k$  are  $2n \times 2n$  positive semi-definite state weighting matrices, we therefore have the form of  $\mathbf{M}_i(t)$ ,  $i = 2, 3, \dots, k$  as follows

$$-\dot{\mathbf{M}}_i(t) = \mathbf{M}_i(t)[\Lambda(\mathbf{Z}) - \mathbf{B}\mathbf{R}_U^{-1}\mathbf{B}^T\mathbf{P}(t)] + [\Lambda(\mathbf{Z}) - \mathbf{B}\mathbf{R}_U^{-1}\mathbf{B}^T\mathbf{P}(t)]^T \mathbf{M}_i(t) + \mathbf{Q}_{Z,i} \quad (21)$$

where the scalar identity Eq. (17) has been used again. It is noted that Eqs. (15) and (21) are the Riccati and Lyapunov matrix equations, respectively. Hence, an optimal polynomial controller is obtained analytically in the form

$$\mathbf{U}(t) = -\mathbf{R}_U^{-1}\mathbf{B}^T\mathbf{P}(t)\mathbf{Z}(t) - \mathbf{R}_U^{-1}\mathbf{B}^T \sum_{i=2}^k [\mathbf{Z}^T(t)\mathbf{M}_i(t)\mathbf{Z}(t)]^{i-1}\mathbf{M}_i(t)\mathbf{Z}(t) \quad (22)$$

It is seen that the polynomial controller consists of linear term and nonlinear term, and the former is the first-order, while the latter is the odd higher-order, e.g. cubic, quintic etc.

One can see that  $\mathbf{P}(t), \mathbf{M}_i(t)$  are both related to the gradient matrix  $\Lambda(\mathbf{Z})$ , indicating that the gain matrices of the polynomial controller  $\mathbf{U}(t)$  need to be calculated in real-time. An approximate solution to the gain matrices is obtained by linearizing the gradient matrix  $\Lambda(\mathbf{Z})$  at the initial equilibrium point  $\mathbf{z}_0$  (Yang *et al.* 1996), i.e., replacing  $\Lambda(\mathbf{Z})$  in Eq. (10) by  $\Lambda_0$ ,  $\Lambda_0 = \Lambda(\mathbf{Z})|_{\mathbf{z}_0}$ . Furthermore, the Riccati matrix  $\mathbf{P}(t)$  and the Lyapunov  $\mathbf{M}_i(t)$  matrices, to a class of optimal control system with time-infinite, could be approximately evaluated as constant matrices  $\mathbf{P}, \mathbf{M}_i$  by solving the following algebraic Riccati and Lyapunov equations, i.e. the steady-state Riccati and Lyapunov matrix equations, respectively

$$\mathbf{P}\Lambda_0 + \Lambda_0^T\mathbf{P} - \mathbf{P}\mathbf{B}\mathbf{R}_U^{-1}\mathbf{B}^T\mathbf{P} + \mathbf{Q}_Z = \mathbf{0} \quad (23)$$

$$\mathbf{M}_i(\Lambda_0 - \mathbf{B}\mathbf{R}_U^{-1}\mathbf{B}^T\mathbf{P}) + (\Lambda_0 - \mathbf{B}\mathbf{R}_U^{-1}\mathbf{B}^T\mathbf{P})^T\mathbf{M}_i + \mathbf{Q}_{Z,i} = \mathbf{0}, \quad i = 2, 3, \dots, k \quad (24)$$

The Eqs. (23) and (24) can be solved using any well-known numerical algorithms or using toolbox functions available in MATLAB.

### 3. Probabilistic solutions of controlled systems

It is seen that all the randomness involved in the above controlled system arises since stochastic parameter vector  $\Theta$ . Hence, the augmented systems constructed by the state and control force components  $(Z(t), \Theta), (U(t), \Theta)$  satisfy the following generalized density evolution equations (GDEEs, Li *et al.* 2010a), respectively

$$\frac{\partial p_{Z\Theta}(z, \theta, t)}{\partial t} + \dot{Z}(\theta, t) \frac{\partial p_{Z\Theta}(z, \theta, t)}{\partial z} = 0 \quad (25)$$

$$\frac{\partial p_{U\Theta}(u, \theta, t)}{\partial t} + \dot{U}(\theta, t) \frac{\partial p_{U\Theta}(u, \theta, t)}{\partial u} = 0 \quad (26)$$

The corresponding instantaneous PDFs of  $Z(t)$  and  $U(t)$  can be obtained by solving a family of partial differential equations with given initial condition, as follows

$$p_{Z\Theta}(z, \theta, t)|_{t=0} = \delta(z - z_0)p_{\Theta}(\theta) \quad (27)$$

$$p_{U\Theta}(u, \theta, t)|_{t=0} = \delta(u - u_0)p_{\Theta}(\theta) \quad (28)$$

where  $\delta(\cdot)$  is the Dirac-Delta function;  $z_0, u_0$  are determinative initial values of  $Z(t), U(t)$ , respectively. We then have

$$p_Z(z, t) = \int_{\Omega_{\Theta}} p_{Z\Theta}(z, \theta, t) d\theta \quad (29)$$

$$p_U(u, t) = \int_{\Omega_{\Theta}} p_{U\Theta}(u, \theta, t) d\theta \quad (30)$$

The joint PDFs  $p_{z\Theta}(z, \theta, t)$  and  $p_{u\Theta}(u, \theta, t)$  are the solutions of Eqs. (25) and (26), respectively, of which the numerical solving procedure involves (Li and Chen 2009): (i) Probability-assigned space partition to determine the representative point set and the assigned probabilities. The strategy via tangent spheres is employed herein (Chen and Li 2008); (ii) Deterministic dynamic response analysis of the system Eq. (1) using a time integration method; (iii) Using the finite difference method to solve the generalized density evolution equations whereby a modified Lax-Wendroff scheme with TVD nature is employed (Chen and Li 2005).; (iv) Numerical integration in Eqs. (29) and (30) to compute the PDFs of interest.

#### 4. Generalized optimal control policy based controller design

There are two typical issues in structural optimal controls, including the identification of the suitable parameters for controllers, e.g. the weighting matrices  $\mathbf{Q}_Z$  and  $\mathbf{R}_U$  in Eq. (22), and the allocation of controllers constrained by the finiteness of available resources. Some freedom towards alleviating the burden of these constraints can be gained by allowing a finite number of controllers to be arbitrarily located in space, and considering the problem of optimal control placement. This controller allocation, however, has not been as extensively investigated as the problem of control force optimization (Amini and Tavassoli 2005). The generalized optimal control policy, therefore, was newly proposed including the optimal parameters and the optimal placements of controllers (Peng *et al.* 2010), which will be used in the following numerical examples.

In order to identify the optimal placements of controllers, a controllability index in the exceedance probability of quantities of interest is defined as

$$\rho_i = \frac{1}{2} [\Pr_{\tilde{Z}_i}^T(\tilde{Z}_i - \tilde{Z}_{i,thd} > \mathbf{0}) \mathbf{Q}_{\tilde{Z}_i} \Pr_{\tilde{Z}_i}(\tilde{Z}_i - \tilde{Z}_{i,thd} > \mathbf{0}) + \Pr_{\tilde{U}_i}^T(\tilde{U}_i - \tilde{U}_{i,thd} > \mathbf{0}) \mathbf{R}_{\tilde{U}_i} \Pr_{\tilde{U}_i}(\tilde{U}_i - \tilde{U}_{i,thd} > \mathbf{0})] \quad (31)$$

$$i = 1, 2, \dots, n$$

where  $\tilde{Z}_i = [\max_t |X_i(\Theta, t)| \max_t |\dot{X}_i(\Theta, t)| \max_t |\ddot{X}_i(\Theta, t)|]^T$ ,  $\tilde{U}_i = \max_t |U_i(\Theta, t)|$  are the extreme-value state and control force vectors at the interval  $[t_0 \ t_f]$ , respectively;  $\Pr(\cdot)$  operates component-wise on its vector argument;  $\tilde{Z}_{i,thd}$ ,  $\tilde{U}_{i,thd}$  are the threshold vectors corresponding to  $\tilde{Z}_i$ ,  $\tilde{U}_i$ . The weighting matrices  $\mathbf{Q}_{\tilde{Z}_i}$ ,  $\mathbf{R}_{\tilde{U}_i}$  denote the relative importance between the state and control force vectors. It is noted that the weighting matrices  $\mathbf{Q}_{\tilde{Z}_i}$ ,  $\mathbf{R}_{\tilde{U}_i}$  here are not same to the weighting matrices  $\mathbf{Q}_Z$ ,  $\mathbf{R}_U$  of Eq. (6), in that they have different units and dimensions. Specifically,  $\mathbf{Q}_{\tilde{Z}_i}$ ,  $\mathbf{R}_{\tilde{U}_i}$  are defined as

$$\mathbf{Q}_{\tilde{Z}_i} = \begin{bmatrix} 1 & 0 & 0 \\ 0 & 1 & 0 \\ 0 & 0 & 1 \end{bmatrix}, \quad \mathbf{R}_{\tilde{U}_i} = [1] \quad (32)$$

Moreover, a controllability index gradient is defined as

$$\Delta \rho_i^j = \frac{\rho_i^{j-1} - \rho_i^j}{\rho_i^{j-1}}, \quad i = 1, 2, \dots, n; j = 1, 2, \dots, r \quad (33)$$

where  $\rho_i^0$  represents the controllability index of the uncontrolled structure. It is noted that the

structural topology is always updated with the newly added proper controller  $j$ . The next controller will be placed at the storey with the minimum of gradient vector  $(\Delta\rho_1^j, \Delta\rho_2^j, \dots, \Delta\rho_n^j)$ , and is ready to prompt an update controller topology until the predetermined objective performance is achieved.

In addition, a performance function can be constructed in the exceedance probability of quantities of interest so as to identify the optimal parameters of controllers, namely

$$J_2(\tilde{Z}, \tilde{U}) = \frac{1}{2} [\Pr_{\tilde{Z}}^T(\tilde{Z} - \tilde{Z}_{thd} > \mathbf{0}) \mathbf{Q}_{\tilde{Z}} \Pr_{\tilde{Z}}(\tilde{Z} - \tilde{Z}_{thd} > \mathbf{0}) + \Pr_{\tilde{U}}^T(\tilde{U} - \tilde{U}_{thd} > \mathbf{0}) \mathbf{R}_{\tilde{U}} \Pr_{\tilde{U}}(\tilde{U} - \tilde{U}_{thd} > \mathbf{0})] \quad (34)$$

where  $\tilde{Z} = [\max_i(\max_t |X_i(\Theta, t)|) \max_i(\max_t |\dot{X}_i(\Theta, t)|) \max_i(\max_t |\ddot{X}_i(\Theta, t)|)]^T$ ,  $\tilde{U} = [\max_i(\max_t |U_i(\Theta, t)|)]$  are equivalent extreme-value vectors of the state and control force at the interval  $[t_0, t_f]$ , respectively;  $\tilde{Z}_{thd}$ ,  $\tilde{U}_{thd}$  are the threshold vectors corresponding to  $\tilde{Z}$ ,  $\tilde{U}$ . It is clear that the exceedance probability performance function has the same physical meaning as the defined controllability index. The weighting matrices  $\mathbf{Q}_{\tilde{Z}}$ ,  $\mathbf{R}_{\tilde{U}}$  are the same as  $\mathbf{Q}_{Z_j}$ ,  $\mathbf{R}_{U_j}$  of Eq. (31). The optimal parameters of newly added controllers, thereby, are obtained by minimizing the performance function in exceedance probability at each stage.

It is well-understood that the state quantities  $\tilde{Z}_i$ ,  $\tilde{Z}$  and the control force quantities  $\tilde{U}_i$ ,  $\tilde{U}$  are governed by the GDEEs, Eqs. (25) and (26), respectively. The exceedance probability of system quantities in the controllability index  $\rho_i$  and in the performance function  $J_2$  can be readily obtained.

The typical form of the generalized optimal control policy is represented by

$$\mathbf{U}(\Theta, t) = \mathbf{f}(\mathbf{I}^*, \mathbf{L}^*) \mathbf{f}(\ddot{\mathbf{X}}, \dot{\mathbf{X}}, \mathbf{X}) \quad (35)$$

where the matrix function  $\mathbf{f}(\mathbf{I}^*, \mathbf{L}^*)$  describes the dependence of the system dynamics on system parameters and control layout. The control force is obtained as matrix  $\mathbf{f}(\mathbf{I}^*, \mathbf{L}^*)$  operates on the state vector, as indicated in Eq. (35). Here,  $\mathbf{I}^* = [I_{\tilde{\mathbf{M}}}^*, I_{\tilde{\mathbf{C}}}^*, I_{\tilde{\mathbf{K}}}^*]$  is the optimal parameter vector denoting the generalized mass  $\tilde{\mathbf{M}}$ , generalized damping  $\tilde{\mathbf{C}}$  and generalized stiffness  $\tilde{\mathbf{K}}$ ;  $\mathbf{L}^* = [L_x^*, L_y^*, L_z^*]$  is optimal topology matrix denoting the control devices distributed in system space with respect to dimensions  $x$ ,  $y$  and  $z$ . The key effort, therefore, is to construct the parameter vector  $(\mathbf{I}^*, \mathbf{L}^*)$  of the matrix function  $\mathbf{f}(\mathbf{I}^*, \mathbf{L}^*)$ .

The details of resolution procedure of the generalized optimal control policy is referred to the previous investigation on linear stochastic optimal control strategy (Peng *et al.* 2010). We attempt to introduce the generalized optimal control policy into the nonlinear stochastic optimal control strategy of hysteretic structures in the following section, and to achieve the desirable structural performance with the maximum of control effectiveness by reasonably designing controllers.

## 5. Numerical examples

The vector form of controlled hysteretic structures subjected to the stochastic external excitation is given by

$$\mathbf{M}\ddot{\mathbf{X}}(t) + \mathbf{C}_t\dot{\mathbf{X}}(t) + \mathbf{R}_t(\mathbf{X}, \mathbf{z}) = \mathbf{B}_s\mathbf{U}(t) + \mathbf{D}_s\mathbf{F}(\varpi, t), \quad \mathbf{X}(t_0) = \mathbf{0}; \quad \dot{\mathbf{X}}(t_0) = \mathbf{0} \quad (36)$$

where  $\mathbf{C}_t$  is the instantaneous damping matrix;  $\mathbf{R}_t(\mathbf{X}, \mathbf{z})$  is an  $n$ -dimensional vector denoting the restoring force, including elastic force and hysteretic force induced by hysteretic displacement  $\mathbf{z}$ .

The restoring force can be partitioned into linear part and hysteretic part

$$\mathbf{R}_t(\mathbf{X}, \mathbf{z}) = \alpha \mathbf{K}_0 \mathbf{X} + (1 - \alpha) \mathbf{K}_0 \mathbf{z} \quad (37)$$

where  $\alpha$  is the stiffness ratio of post-yielding to pre-yielding;  $\mathbf{K}_0$  is the pre-yielding stiffness matrix.

Using the Maclaurin series Eq. (3), the equation of controlled hysteretic structures can be re-written as the state space form

$$\begin{aligned} \dot{\mathbf{Z}}(t) &= \Lambda(\mathbf{Z})\mathbf{Z}(t) + \mathbf{B}\mathbf{U}(t) + \mathbf{D}\mathbf{F}(\varpi, t) \quad (38) \\ \mathbf{Z}(t) &= \begin{bmatrix} \mathbf{X}(t) \\ \dot{\mathbf{X}}(t) \end{bmatrix}, \quad \mathbf{B} = \begin{bmatrix} \mathbf{0} \\ \mathbf{M}^{-1} \mathbf{B}_s \end{bmatrix}, \quad \mathbf{D} = \begin{bmatrix} \mathbf{0} \\ \mathbf{M}^{-1} \mathbf{D}_s \end{bmatrix} \\ \Lambda(\mathbf{Z}) &= \begin{bmatrix} \mathbf{0} & \mathbf{I} \\ -\mathbf{M}^{-1} \left( \alpha \mathbf{K}_0 + (1 - \alpha) \mathbf{K}_0 \sum_{i=1}^m \frac{\mathbf{X}^{i-1}}{i!} \frac{\partial^i \mathbf{z}(0)}{\partial \mathbf{X}^i} \right) & -\mathbf{M}^{-1} \mathbf{C}_l \end{bmatrix}, \quad \Lambda_0 = \begin{bmatrix} \mathbf{0} & \mathbf{I} \\ -\alpha \mathbf{M}^{-1} \mathbf{K}_0 & -\mathbf{M}^{-1} \mathbf{C}_0 \end{bmatrix} \quad (39) \end{aligned}$$

where  $\mathbf{C}_0$  is the pre-yielding damping matrix.

It is noted that the functional expression of hysteretic displacement  $\mathbf{z}$  represents the type of hysteretic forces. Two numerical examples including a ten-storey shear frame and an eight-storey shear frame controlled by active tendons are investigated, of which the hysteretic forces are described by Clough bilinear model and Bouc-Wen differential model, respectively. The weighting matrices of active control actions can be approximately expressed as the diagonal matrices, since their diagonal elements are usually far larger than the off-diagonal elements (Chen *et al.* 1992)

$$\mathbf{Q} = \text{diag}\{Q_{d_1}, \dots, Q_{d_n}, Q_{v_1}, \dots, Q_{v_n}\}, \quad \mathbf{R} = \text{diag}\{R_{u_1}, \dots, R_{u_r}\} \quad (40)$$

A physical stochastic ground motion model  $\ddot{x}_g(\Theta, t)$  is employed as the random excitation of the exemplified systems,  $\Theta = \{\Theta_{\omega_0}, \Theta_{\zeta}, \Theta_b\}$ , where  $\Theta_{\omega_0}, \Theta_{\zeta}$  are the random parameters denoting the predominant frequency and the equivalent damping ratio of a certain engineering site soil, respectively;  $\Theta_b$  is the random vector characterizing the randomness involved in the ground motion at the bedrock coming from the properties of the sources and the propagation path (Li and Ai 2006, Chen *et al.* 2007). The peak acceleration of the motion is defined as 0.3 g. A representative time histories are illustrated in Fig. 1.

The generalized optimal control policy is employed to design the active tendons, and the objective of the control design is to effectively improve the hysteretic structural performance by reasonably distributing a few of controllers (six controllers in example 1 and five controllers in example 2) and constructing the optimal weighting matrices of their control gains. As a comparative case, the hysteretic systems with the same number controllers are investigated, of which the controllers are placed from the ground floor to upper floors, and their controller parameters are designed as the same.

The optimization method used in choosing weighting matrices is the quasi-Newton based OPT++, a toolbox function of DAKOTA (Eldred *et al.* 2007).

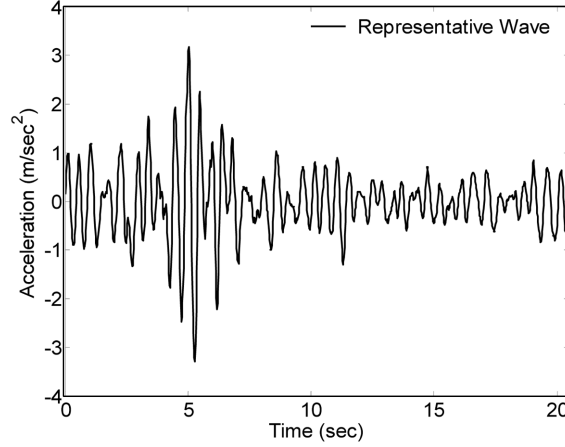


Fig. 1 Numerical examples: a representative time histories of ground acceleration

### 5.1 Example 1: ten-storey shear frame with clough bilinear model

The restoring force of the shear frame described by Clough bilinear model is in the form

$$\mathbf{R}_t(\mathbf{X}, \mathbf{z}) = \mathbf{K}_t \mathbf{X} \quad (41)$$

The storey mass and storey stiffness of the exemplified ten-storey shear frame are shown in Table 1. Rayleigh's damping  $\mathbf{C}_t = a\mathbf{M} + b\mathbf{K}_t$ , where  $a = 0.01$ ,  $b = 0.005$ , is employed, resulting in a damping ratio of 1.01% for the first vibrational mode. The natural frequencies of the unyielded building are respectively 3.46, 10.00, 15.83, 21.26, 26.57, 31.39, 35.25, 38.64, 41.33, and 44.44 rad/sec. The restoring force relationship of each inter-storey is shown in Fig. 2, with the uniform stiffness ratio  $\alpha = 0.1$ , while the initial yielding displacements  $\Delta_y$  of each storey are listed in Table 1, by which the instantaneous stiffness  $\mathbf{K}_t$  could be evaluated. The thresholds of the structural inter-storey drifts, inter-storey velocities, storey accelerations and the control forces are 15 mm, 150 mm/sec, 8000 mm/sec<sup>2</sup> and 200 kN, respectively. The deterministic non-linear dynamic analysis of the bilinear hysteretic system, involved in solving the generalized density evolution equations, resorts to the Newmark- $\beta$  time integration (Clough and Penzien 1993).

The optimal placement and weight matrices of newly added active tendon with a first-order term in each sequence case are shown in Table 2. It is seen that the six controllers are distributed in the inter-9-10-storey, the inter-6-7-storey, the inter-5-6-storey, the inter-7-8-storey, the inter-4-5-storey,

Table 1 Numerical example 1: parameters of the ten-storey shear frame

Storey	0-1	1-2	2-3	3-4	4-5	5-6	6-7	7-8	8-9	9-10
Mass ( $1 \times 10^4$ kg)	2.4	2.4	2.0	2.0	1.8	1.8	1.6	1.6	1.2	1.2
Pre-yielding Stiffness (kN/mm)	18	18	14	14	12	12	10	10	9.6	9.6
$\Delta_y$ (mm)	10.0	10.0	8.0	8.0	8.0	8.0	8.0	8.0	6.0	6.0

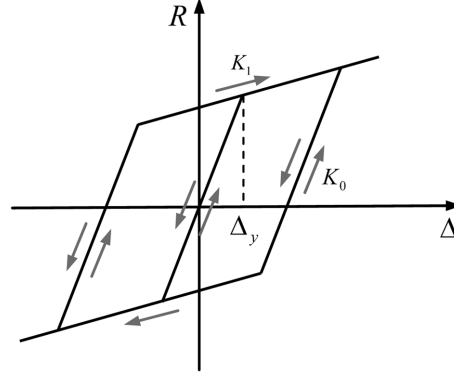


Fig. 2 Numerical example 1: Clough bilinear hysteretic restoring force model

Table 2 Numerical example 1: optimal parameters of tendons of the controlled hysteretic system with Clough bilinear model

Sequence no.	Topology vector	Parameters of appending weighting matrices*						
		$Q_d$	$Q_v$	$Q_{d,2}$	$Q_{v,2}$	$Q_{d,3}$	$Q_{v,3}$	$R_u$
0	$[0\ 0\ 0\ 0\ 0\ 0\ 0\ 0\ 0\ 0]^T$	--	--	--	--	--	--	--
1 (1st order)	$[0\ 0\ 0\ 0\ 0\ 0\ 0\ 0\ 0\ 1]^T$	187.2	0.0	--	--	--	--	$10^{-10}$
2 (1st order)	$[0\ 0\ 0\ 0\ 0\ 0\ 2\ 0\ 0\ 1]^T$	84.3	217.5	--	--	--	--	$10^{-10}$
3 (1st order)	$[0\ 0\ 0\ 0\ 0\ 3\ 2\ 0\ 0\ 1]^T$	207.9	0.0	--	--	--	--	$10^{-10}$
4 (1st order)	$[0\ 0\ 0\ 0\ 0\ 3\ 2\ 4\ 0\ 1]^T$	0.0	532.2	--	--	--	--	$10^{-10}$
5 (1st order)	$[0\ 0\ 0\ 0\ 5\ 3\ 2\ 4\ 0\ 1]^T$	73.3	0.0	--	--	--	--	$10^{-10}$
6 (1st order)	$[0\ 0\ 6\ 0\ 5\ 3\ 2\ 4\ 0\ 1]^T$	0.0	62.3	--	--	--	--	$10^{-10}$
6 (3rd order)	$[0\ 0\ 6\ 0\ 5\ 3\ 2\ 4\ 0\ 1]^T$	0.0	62.3	0.0	0.0	--	--	$10^{-10}$
6 (5th order)	$[0\ 0\ 6\ 0\ 5\ 3\ 2\ 4\ 0\ 1]^T$	0.0	62.3	0.0	0.0	0.0	1.8	$10^{-10}$
Comparative case	$[1\ 2\ 3\ 4\ 5\ 6\ 0\ 0\ 0\ 0]^T$	300.0	0.0	--	--	--	--	$10^{-10}$

\*Initial values of parameters are  $Q_d = Q_v = 100$ ,  $Q_{d,2} = Q_{v,2} = 5$ ,  $Q_{d,3} = Q_{v,3} = 2$ ,  $R_u = 10^{-10}$ .

and the inter-2-3-storey in turn, respectively. Thus, the parameter vector in the matrix function of generalized optimal control policy is given by

$$(Q_d^*, Q_v^*, R_u^*, L^*) = \begin{bmatrix} 0 & 0 & 0.0 & 0 & 73.3 & 207.9 & 84.3 & 0.0 & 0 & 187.2 \\ 0 & 0 & 62.3 & 0 & 0.0 & 0.0 & 217.5 & 532.2 & 0 & 0.0 \\ 0 & 0 & 10^{-10} & 0 & 10^{-10} & 10^{-10} & 10^{-10} & 10^{-10} & 0 & 10^{-10} \\ 0 & 0 & 6 & 0 & 5 & 3 & 2 & 4 & 0 & 1 \end{bmatrix}^T \quad (42)$$

The active tendons with higher-order terms, e.g., 3rd-order and 5th-order, are investigated to further improve the structural performance. For convenience of optimization, the unified weighting matrices are arranged to the higher-order terms of all controllers. The optimal weighting matrices of higher-order terms are also shown in Table 2. It is seen the higher-order weighting matrices almost all equal to zero, indicating that the higher-order terms do not contribute to improve the structural

Table 3 Numerical example 1: optimization results of the hysteretic system with Clough bilinear model controlled by 1st order controllers

Sequence no.	Topology vector	Exceedance probabilities				Objective function $J_2$
		$P_{f,\tilde{x}}$	$P_{f,\tilde{\dot{x}}}$	$P_{f,\tilde{\ddot{x}}}$	$P_{f,\tilde{u}}$	
0	$[0\ 0\ 0\ 0\ 0\ 0\ 0\ 0\ 0\ 0]^T$	0.5016	0.6032	0.7829	--	0.6142
1	$[0\ 0\ 0\ 0\ 0\ 0\ 0\ 0\ 0\ 1]^T$	0.4942	0.5822	0.7685	$3.600 \times 10^{-7}$	0.5869
2	$[0\ 0\ 0\ 0\ 0\ 0\ 2\ 0\ 0\ 1]^T$	0.4355	0.5420	0.7597	0.0268	0.5306
3	$[0\ 0\ 0\ 0\ 0\ 3\ 2\ 0\ 0\ 1]^T$	0.3927	0.5152	0.7573	0.0364	0.4973
4	$[0\ 0\ 0\ 0\ 0\ 3\ 2\ 4\ 0\ 1]^T$	0.3694	0.4330	0.7534	0.1859	0.4630
5	$[0\ 0\ 0\ 0\ 5\ 3\ 2\ 4\ 0\ 1]^T$	0.3580	0.4091	0.7511	0.0326	0.4304
6	$[0\ 0\ 6\ 0\ 5\ 3\ 2\ 4\ 0\ 1]^T$	0.3527	0.3918	0.7497	0.0705	0.4225
Comparative case	$[1\ 2\ 3\ 4\ 5\ 6\ 0\ 0\ 0\ 0]^T$	0.3952	0.5178	0.7596	0.0221	0.5009

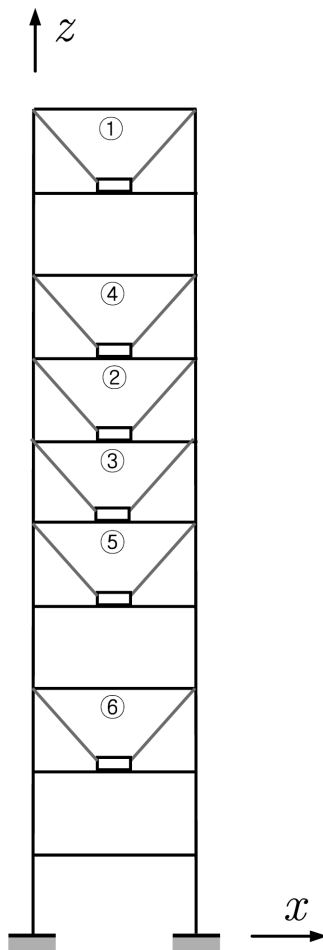


Fig. 3 Numerical example 1: tendons placement using storey controllability gradient criterion

performance. This reveals that the linear control with the 1st-order controller suffices even for the nonlinear systems when the exceedance probability based control criterion for designing the optimal weighting matrices is employed. This is practically meaningful since it bypasses the need to utilize nonlinear controllers which may be associated with dynamical instabilities. It does not follow the traditional knowledge that nonlinear optimal control is more robust and more effective than the linear optimal control in the context of deterministic control (Bernstein 1993).

The exceedance probabilities of quantities and the objective function are presented in Table 3. The table reveals that the exceedance probabilities of quantities are gradually reduced with the optimal placement and design of tendons, and they reach to the minimum until all the six controllers are placed. Fig. 3 shows the placement of tendons, indicated as the numbers in the structural stories. Compared with the comparative case, one might see that using only 3 tendons can reach to the same control effectiveness, indicating the validity and applicability of the generalized optimal control policy.

Time histories of the mean and standard deviation of the inter-storey drifts of the 1st and 10th storey with and without control are shown in Fig. 4. It is clear that the response processes of the controlled system have a certain extent of reduction compared with those of the uncontrolled system. The storey acceleration, however, does not get obvious improvement; see Fig. 5, the time histories of the mean and the standard deviation of storey accelerations of the 1st and 10th storey with and without control. It is understood that the filter function of nonlinear systems to the ground motion becomes weaker due to the interaction of control force.

Figs. 6-9 further show the PDFs at typical instants of time of inter-storey drifts and storey accelerations of the 1st and 10th storey with and without control. One might see that the distribution range of the PDFs of controlled inter-storey drifts becomes narrower than that of the uncontrolled inter-storey drifts. The PDFs of storey accelerations, meanwhile, have not obvious improvement compared with those of uncontrolled storey accelerations, which is corresponding to the behavior of second-order moment shown in Fig. 5. It is also indicated that the shear frame structure does not move as the similar profile after it is controlled due to the effect of the control force, since the PDF

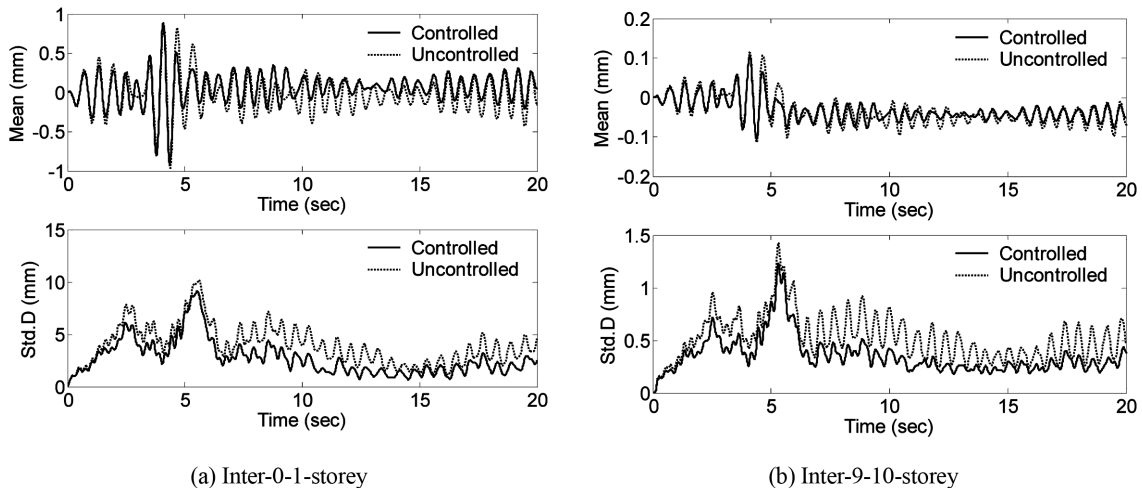


Fig. 4 Numerical example 1: time histories of mean and standard deviation of inter-storey drifts with/without control

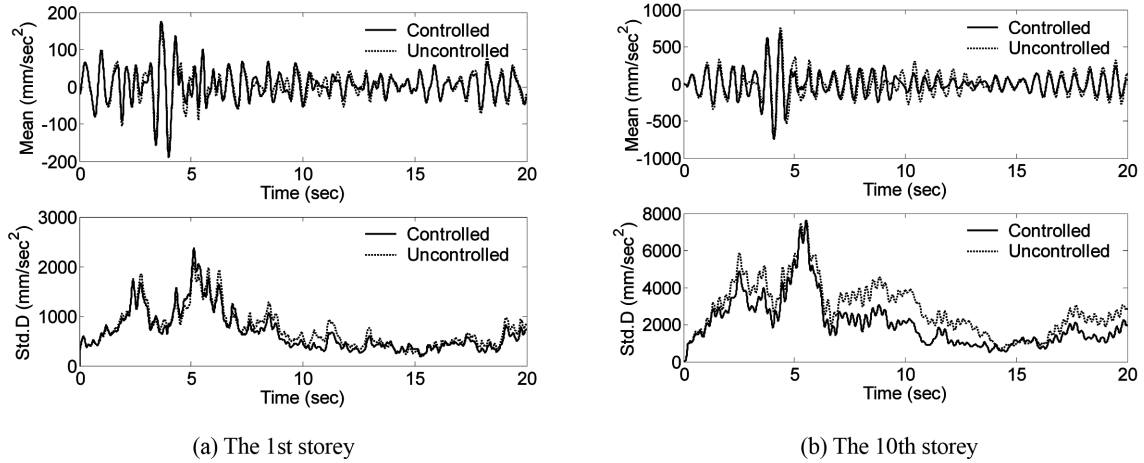


Fig. 5 Numerical example 1: time histories of mean and standard deviation of storey accelerations with/without control

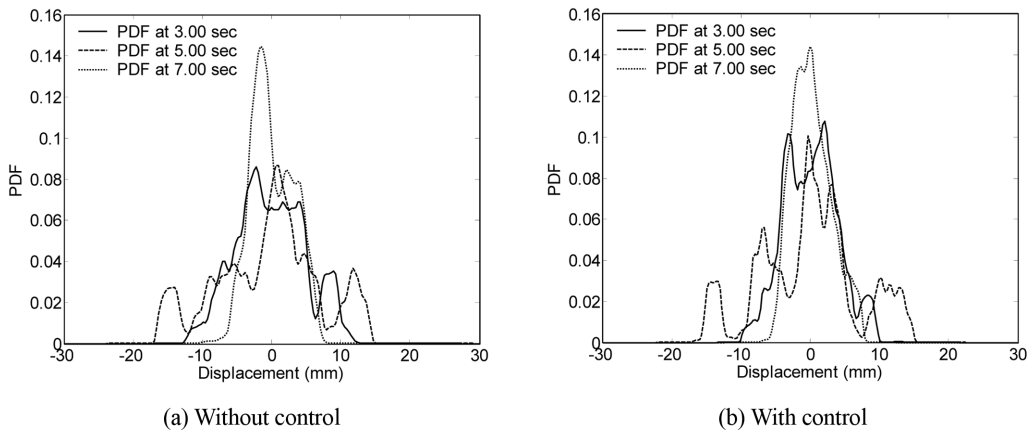


Fig. 6 Numerical example 1: typical PDFs of the inter-0-1-storey drift at certain instants of time

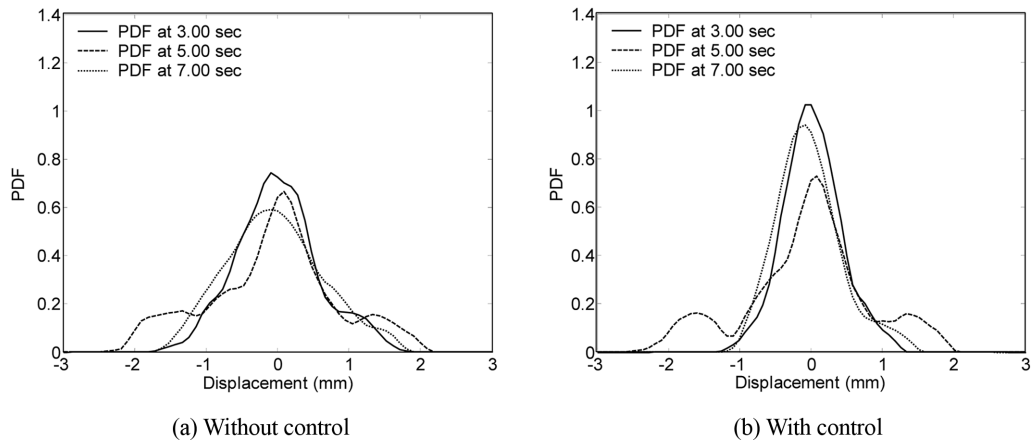


Fig. 7 Numerical example 1: typical PDFs of the inter-9-10-storey drift at certain instants of time

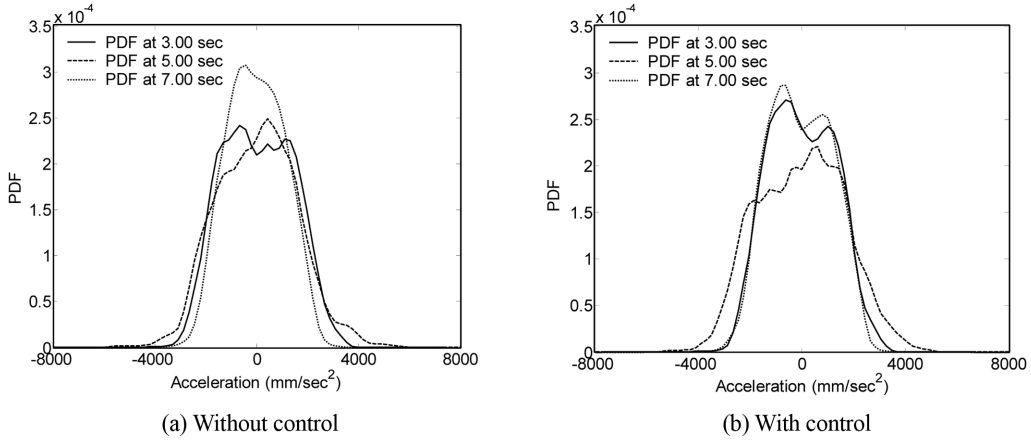


Fig. 8 Numerical example 1: typical PDFs of the 1st storey acceleration at certain instants of time

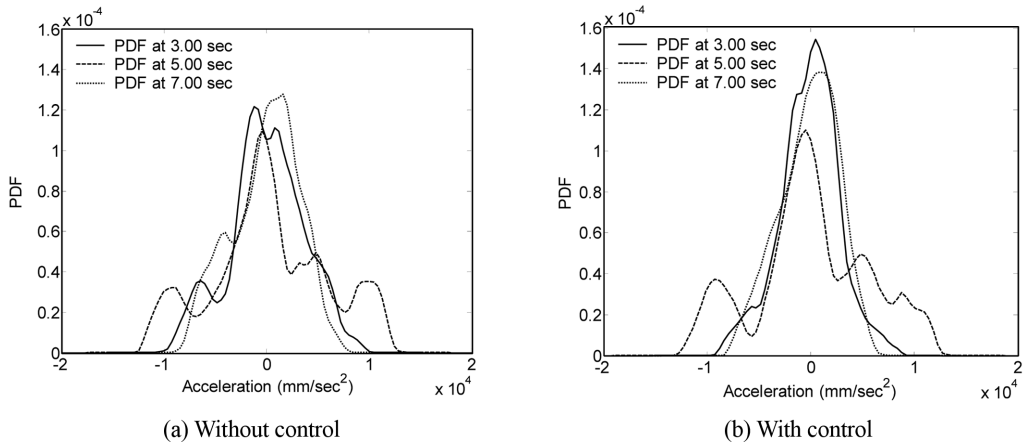


Fig. 9 Numerical example 1: typical PDFs of the 10th storey acceleration at certain instants of time

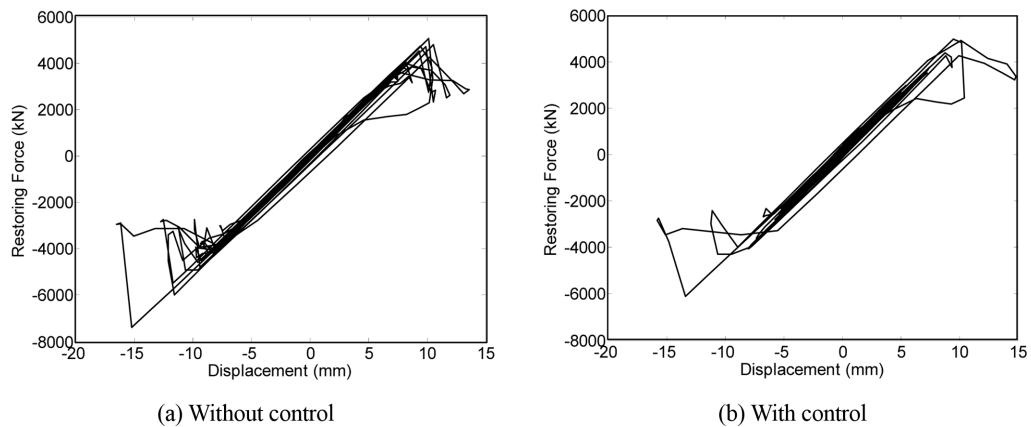


Fig. 10 Numerical example 1: the hysteretic curves of the inter-0-1-storey component under a representative ground motion

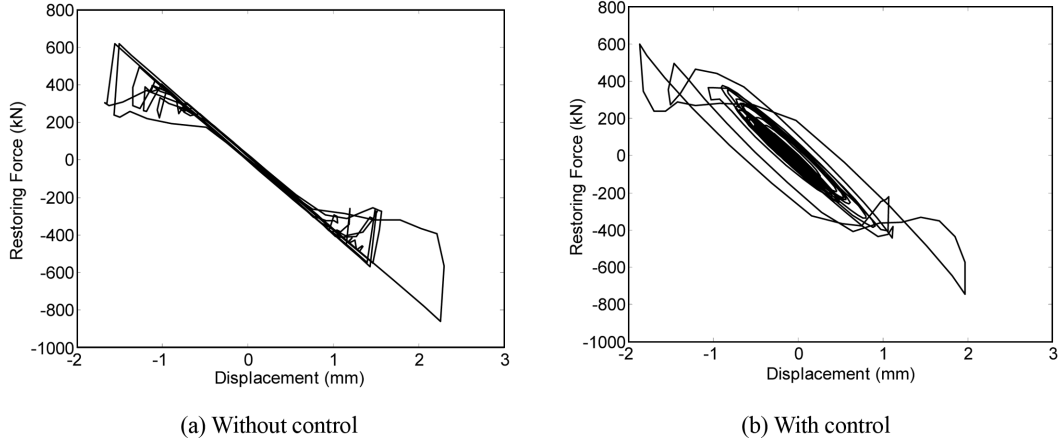


Fig. 11 Numerical example 1: the hysteretic curves of the inter-9-10-storey component under a representative ground motion

curve shapes of the controlled system quantities of interest are different from those of the uncontrolled system quantities.

The hysteretic behaviors of structural components located in the inter-0-1-storey and the inter-9-10-storey under a typical representative ground motion are shown in Fig. 10 and Fig. 11. It is seen that the inter-stories of the controlled structure become smaller than those of the uncontrolled structure. The restoring forces of components also become smaller due to the compensation of external control forces. The hysteretic curve shapes of the controlled components are similar to those of the uncontrolled components. The difference between them is that the energy dissipation of the controlled structure mainly derives from the component cycle motion in a smaller range. It is noted that the controlled structural response is referred to be the component motion around the equilibrium point.

### 5.2 Example 2: eight-storey shear frame with bouc-wen differential model

The structural parameters of the other exemplified eight-storey shear frame are follows:  $m_1 = m_2 = 1.0 \times 10^5$  kg,  $m_3 = m_4 = 0.9 \times 10^5$  kg,  $m_5 = m_6 = 0.9 \times 10^5$  kg,  $m_7 = m_8 = 0.8 \times 10^5$  kg;  $k_1 = k_2 = 3.6 \times 10^1$  kN/mm,  $k_3 = k_4 = 3.2 \times 10^1$  kN/mm,  $k_5 = k_6 = 3.2 \times 10^1$  kN/mm,  $k_7 = k_8 = 2.8 \times 10^1$  kN/mm. Rayleigh's damping  $\mathbf{C} = a\mathbf{M} + b\mathbf{K}$  is employed, where  $a = 0.01$ ,  $b = 0.005$ , resulting in a damping ratio of 1.05% for the first vibrational mode. The natural frequencies of the unyielded building are respectively 3.64, 10.40, 16.46, 22.45, 27.91, 31.89, 34.68, and 36.81 rad/sec. Referring to the basic shape of Osgood-Ramberg model, Bouc proposed a differential equation with smooth hysteretic displacement

$$\dot{z} = A\dot{x} - \beta|\dot{x}|z^{n-1} + \gamma\dot{x}|z|^n \quad (43)$$

The classical Bouc-Wen model features hysteretic behaviors of the restoring force (Wen 1976), whereas it is difficult to reflect the strength deterioration, the stiffness degradation and the pinching effect (Ma *et al.* 2004). These features can be characterized by the extended Bouc-Wen models (Foliente 1995), where the component form of hysteretic displacement  $\mathbf{z}$  in Eq. (43) is given by

$$\dot{z} = h(z) \left\{ \frac{A\dot{x} - v(\beta|\dot{x}||z|^{n-1}z + \gamma\dot{x}|z|^n)}{\eta} \right\} \quad (44)$$

in which  $h(z)$ ,  $v$ ,  $\eta$  are parameters characterizing the pinching effect, the strength deterioration and the stiffness degradation, respectively. These parameters all are dependent on nonlinearities evolution history of the investigated system, and generally related to energy dissipation. An index denoting energy dissipation can be defined as

$$\varepsilon(t) = \int_0^t z\dot{x}dt \quad (45)$$

we then have

$$v(\varepsilon) = 1 + \delta_v \varepsilon, \quad \eta(\varepsilon) = 1 + \delta_\eta \varepsilon \quad (46)$$

where  $\delta_v$ ,  $\delta_\eta$  are the indices reflecting the strength deterioration and the stiffness degradation.

Further, let

$$h(z) = 1 - \zeta_1 e^{-[z \operatorname{sgn}(\dot{x}) - qz_u]^2 / \zeta_2^2} \quad (47)$$

in which  $z_u$  is the extreme hysteretic displacement component

$$z_u = \left( \frac{1}{v(\beta + \gamma)} \right)^{1/n} \quad (48)$$

while the two parameters  $\zeta_1(\varepsilon)$  and  $\zeta_2(\varepsilon)$  take the forms, respectively

$$\zeta_1(\varepsilon) = \zeta_s (1 - e^{-p\varepsilon}) \quad (49)$$

$$\zeta_2(\varepsilon) = (\psi + \delta_\psi \varepsilon)(\lambda + \zeta_1) \quad (50)$$

The 13 parameters used in the extended Bouc-Wen model take the values as follows:  $\alpha = 0.01$ ,  $A = 1.0$ ,  $\beta = 140.0$ ,  $\gamma = 20.0$ ,  $n = 1.0$ ,  $\delta_v = 0.002$ ,  $\delta_\eta = 0.001$ ,  $\psi = 0.2$ ,  $\delta_\psi = 0.005$ ,  $\lambda = 0.1$ ,  $\zeta_s = 0.95$ ,  $q = 0.25$ ,  $p = 2000.0$ . The thresholds of structural inter-storey drifts, inter-storey velocities, storey accelerations and the control forces are 30 mm, 300 mm/sec, 3000 mm/sec<sup>2</sup> and 200 kN, respectively. The physical ground motions employed in the first example is used here.

An explicit time integration method is employed in the deterministic non-linear dynamic analysis of the hysteretic system

$$\ddot{\mathbf{X}}(k+1) = \mathbf{M}^{-1}[\mathbf{F}(\varpi, k) - \mathbf{C}\dot{\mathbf{X}}(k) - \mathbf{R}_t(\mathbf{X}(k), \mathbf{z}(k))] \quad (51)$$

$$\dot{\mathbf{X}}(k+1) = \dot{\mathbf{X}}(k) + (1 - \gamma_a)\ddot{\mathbf{X}}(k)\Delta t + \gamma_a\ddot{\mathbf{X}}(k+1)\Delta t \quad (52)$$

$$\mathbf{X}(k+1) = \mathbf{X}(k) + \dot{\mathbf{X}}(k)\Delta t + \left(\frac{1}{2} - \beta_a\right)\ddot{\mathbf{X}}(k)\Delta t^2 + \beta_a\ddot{\mathbf{X}}(k+1)\Delta t^2 \quad (53)$$

It is proved that the scheme is second-order accurate when  $\gamma_a = 3/2$ , and unconditionally stable if  $1 \leq \beta_a \leq 28/27$  (Chung and Lee 1994). In addition, the hysteretic displacement  $\mathbf{z}$  can be solved employing the fourth-order Runge-Kutta scheme.

Table 4 shows the optimal placement and weight matrices of newly added active tendon with a first-order term in each sequence case. It is seen that the five controllers are distributed in the inter-0-1-storey, the inter-1-2-storey, the inter-2-3-storey, the inter-3-4-storey and the inter-5-6-storey in turn, respectively. Thus, the parameter vector in the matrix function of generalized optimal control policy is given by

$$(Q_d^*, Q_v^*, R_u^*, L^*) = \begin{bmatrix} 642.5 & 100.2 & 777.9 & 57.1 & 0 & 225.5 & 0 & 0 \\ 73.0 & 47.9 & 485.7 & 1072.0 & 0 & 193.1 & 0 & 0 \\ 10^{-9} & 10^{-9} & 10^{-9} & 10^{-9} & 0 & 10^{-9} & 0 & 0 \\ 1 & 2 & 3 & 4 & 0 & 5 & 0 & 0 \end{bmatrix}^T \quad (54)$$

In order to evaluate the control effectiveness of the 1st-order control, we also investigate the higher-order control of the hysteretic system. The optimal weighting matrices of higher-order terms

Table 4 Numerical example 2: optimal parameters of tendons of the controlled hysteretic system with Bouc-Wen differential model

Sequence no.	Topology vector	Parameters of appending weighting matrices*						
		$Q_d$	$Q_v$	$Q_{d,2}$	$Q_{v,2}$	$Q_{d,3}$	$Q_{v,3}$	$R_u$
0	[0 0 0 0 0 0 0 0] <sup>T</sup>	--	--	--	--	--	--	--
1 (1st order)	[1 0 0 0 0 0 0 0] <sup>T</sup>	642.5	73.0	--	--	--	--	10 <sup>-9</sup>
2 (1st order)	[1 2 0 0 0 0 0 0] <sup>T</sup>	100.2	47.9	--	--	--	--	10 <sup>-9</sup>
3 (1st order)	[1 2 3 0 0 0 0 0] <sup>T</sup>	777.9	485.7	--	--	--	--	10 <sup>-9</sup>
4 (1st order)	[1 2 3 4 0 0 0 0] <sup>T</sup>	57.1	1072.0	--	--	--	--	10 <sup>-9</sup>
5 (1st order)	[1 2 3 4 0 5 0 0] <sup>T</sup>	225.5	193.1	--	--	--	--	10 <sup>-9</sup>
5 (3rd order)	[1 2 3 4 0 5 0 0] <sup>T</sup>	225.5	193.1	0.0	0.0	--	--	10 <sup>-9</sup>
5 (5th order)	[1 2 3 4 0 5 0 0] <sup>T</sup>	225.5	193.1	0.0	0.0	0.0	0.6	10 <sup>-9</sup>
Comparative case	[1 2 3 4 5 0 0 0] <sup>T</sup>	0.0	1027.0	--	--	--	--	10 <sup>-9</sup>

\*Initial values of parameters are  $Q_d = Q_v = 100$ ,  $Q_{d,2} = Q_{v,2} = 20$ ,  $Q_{d,3} = Q_{v,3} = 10$ ,  $R_u = 10^{-9}$ .

Table 5 Numerical example 2: optimization results of hysteretic system with Bouc-Wen differential model controlled by 1st order controllers

Sequence no.	Topology vector	Exceedance probabilities				Objective function $J_2$
		$P_{f,\tilde{x}}$	$P_{f,\tilde{y}}$	$P_{f,\tilde{z}}$	$P_{f,\tilde{u}}$	
0	[0 0 0 0 0 0 0 0] <sup>T</sup>	0.8354	0.1334	0.8441	--	0.7141
1	[1 0 0 0 0 0 0 0] <sup>T</sup>	0.5714	0.0186	0.6867	0.0000	0.3992
2	[1 2 0 0 0 0 0 0] <sup>T</sup>	0.5833	0.0210	0.6252	3.603×10 <sup>-7</sup>	0.3658
3	[1 2 3 0 0 0 0 0] <sup>T</sup>	0.5279	0.0585	0.3917	3.602×10 <sup>-7</sup>	0.2178
4	[1 2 3 4 0 0 0 0] <sup>T</sup>	0.4777	0.0919	0.1846	4.276×10 <sup>-7</sup>	0.1354
5	[1 2 3 4 0 5 0 0] <sup>T</sup>	0.4286	0.0756	0.1740	3.603×10 <sup>-7</sup>	0.1098
Comparative case	[1 2 3 4 5 0 0 0] <sup>T</sup>	0.7125	0.1372	0.1345	0.0041	0.2723

are shown in Table 4. Again, it is seen that the higher-order terms do not contribute to further improve the structural performance, and the corresponding optimal parameters almost all equal to zero, indicating once again that the linear control with 1st-order controller can cover the nonlinear control with higher-order controllers when the exceedance probability based control criterion for designing the weighting matrices is employed, as mentioned in example 1.

Table 5 presents the exceedance probabilities of quantities and the objective function in each

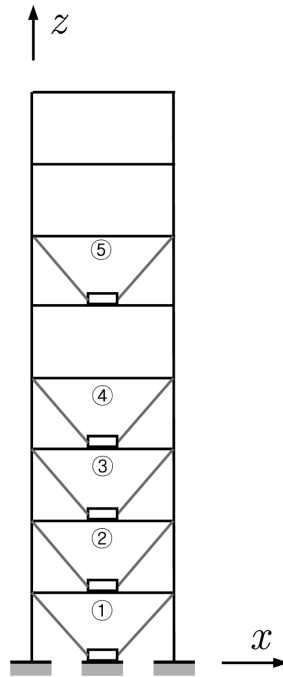


Fig. 12 Numerical example 2: tendons placement using storey controllability gradient criterion

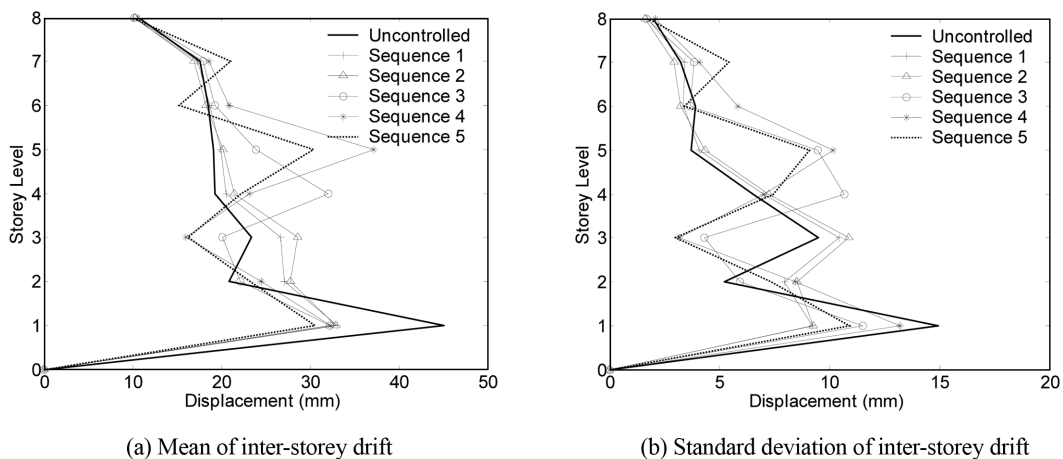


Fig. 13 Numerical example 2: second-order statistics of extreme-value inter-storey drift varying along storey level with the placement of tendons

sequence case. The exceedance probabilities of quantities are gradually reduced with the optimal placement and design of tendons, and they reach to the minimum until all the five controllers are placed. Fig. 12 shows the placement of tendons, indicated as the numbers in the structural stories. Compared with the comparative case, the sequence using only 3 tendons can reach to the same control effectiveness, which is similar to the control effectiveness of example 1.

The second-order statistics of extreme-value inter-storey drifts and extreme-value storey accelerations varying along the height of the structure with the placement of tendons are illustrated in Figs. 13 and 14, respectively. One might see that the means and standard deviations of quantities of interest become smaller with the added tendons, and they are smoother along the height of the structure. It is also seen that too few controllers might result in amplification of the local response of the structure, and meanwhile, the inter-stories with larger responses get more significant improvement. It is noted that the controlled system response results in a desirable structural performance.

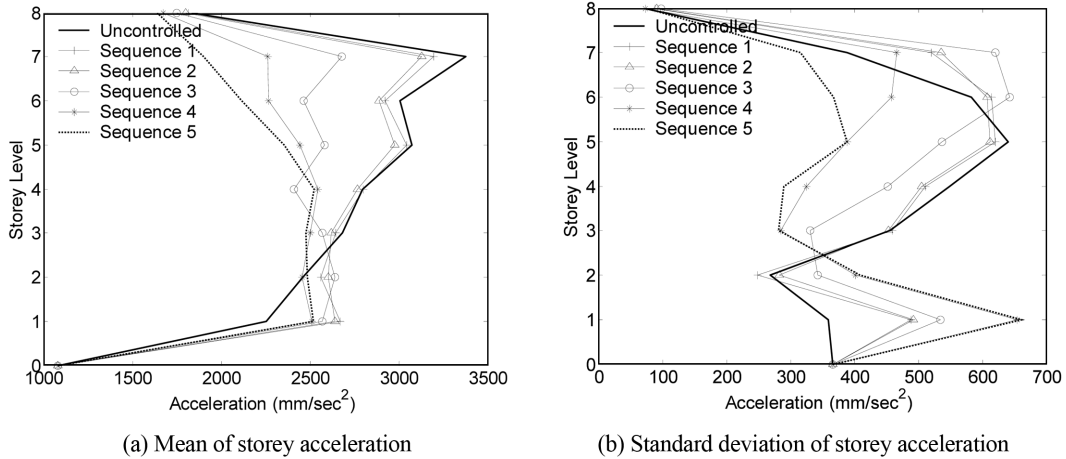


Fig. 14 Numerical example 2: second-order statistics of extreme-value storey acceleration varying along storey level with the placement of tendons

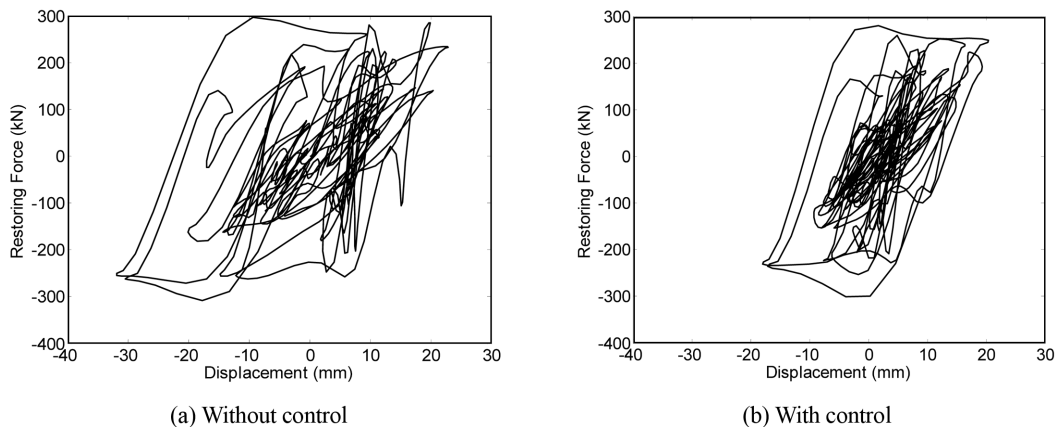


Fig. 15 Numerical example 2: the hysteretic curves of the inter-0-1-storey component under a representative ground motion

The hysteretic behaviors of structural components located in the inter-0-1-storey and the inter-7-8-storey under a typical representative ground motion are shown in Fig. 15 and Fig. 16. It is seen that the hysteretic curves of the uncontrolled components and controlled components feature the Bouc-Wen prosperities, i.e., the strength deterioration, the stiffness degradation and the pinching effect. The inter-storey drifts of the controlled structure become smaller than those of the uncontrolled structure. The restoring forces of components also become smaller due to the compensation of external control forces. The energy dissipation of the controlled structure mainly derives from the component cycle motion in a smaller range. It is noted that the optimal control significantly improves the structural response performance.

Fig. 17 pictures the time histories of root-mean-square hysteretic energy dissipation of the inter-0-1-storey and the inter-7-8-storey. It is seen that the energy dissipations of components at different stories are controlled to a certain extent. Less improvement arises in the first storey where the energy dissipation of the component is both remarkable before or after control. Greater

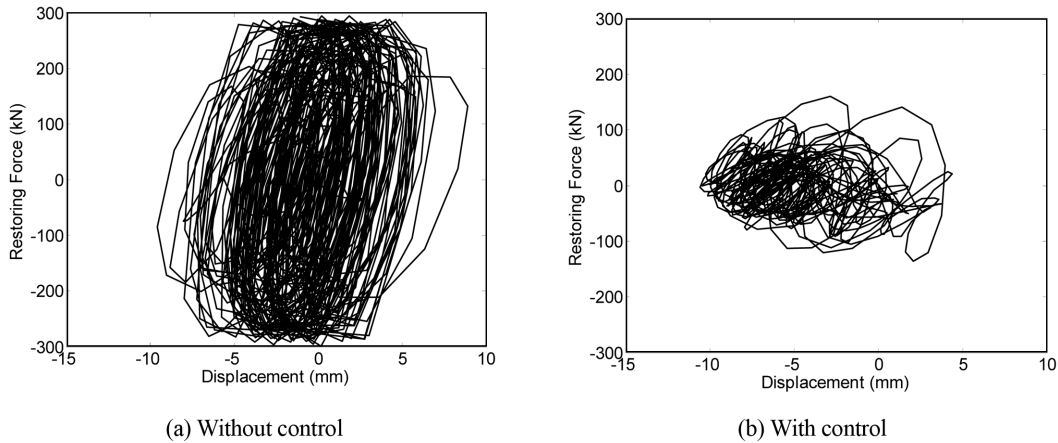


Fig. 16 Numerical example 2: the hysteretic curves of the inter-7-8-storey component under a representative ground motion

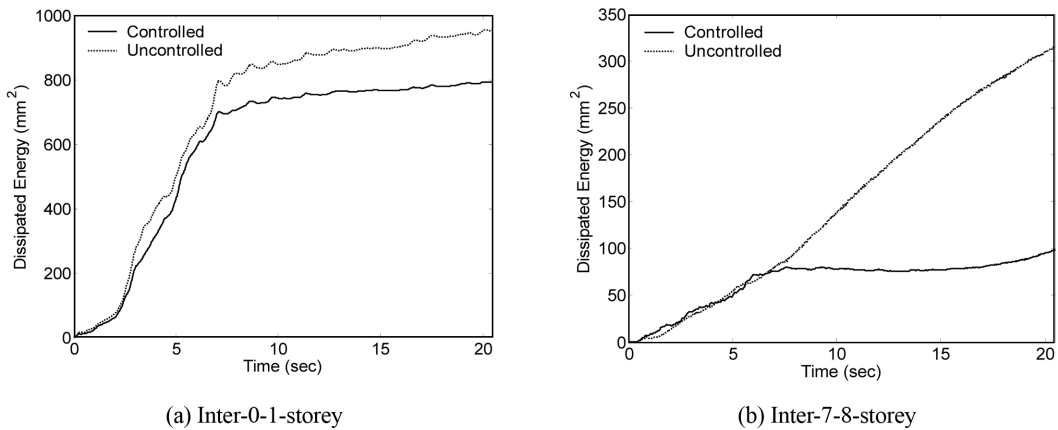


Fig. 17 Numerical example 2: time histories of root-mean-square scaled hysteretic energy dissipation of inter-storey component with/without control

improvement arises in the 8th storey where the energy dissipation of the controlled component evolves in a mild tendency, whereas that of the uncontrolled component goes in a sharply upward tendency.

## 6. Conclusions

A nonlinear stochastic optimal control strategy, in the context of the formulation of physical stochastic optimal control of structures, has been developed for hysteretic structural systems in the present paper. This control strategy is applicable to practically random excitation driven systems. The newly developed generalized optimal control policy is introduced into the nonlinear control scheme to logically distribute the controllers and design their parameters associated with control gains. Numerical investigations of stochastic optimal controls of two base-excited hysteretic structures respectively with Clough bilinear model and Bouc-Wen differential model are carried out for illustrative purposes. The concluding remarks are included as follows:

(1) The linear control with the 1st-order controller suffices even for the hysteretic structural systems when the exceedance probability based control criterion for designing the optimal weighting matrices is employed. This is practically meaningful since it bypasses the need to utilize nonlinear controllers which may be associated with dynamical instabilities.

(2) Using the generalized optimal control policy, a few number of control devices are placed and designed in an efficient mode whereby the maximum control effectiveness can be achieved. It allows for a more desirable structural performance than the controller topology with devices placed from ground floor of the structure.

(3) The nonlinear stochastic optimal control scheme operates efficiently on the hysteretic structural systems. The structural performance, as gaged by the statistics and probability density functions of physical quantities of interest, is improved and meanwhile, energy-dissipation behavior of the hysteretic structures is controlled to a certain extent.

## Acknowledgements

The supports of the National Natural Science Foundation of China for Innovative Research Groups (Grant No. 50621062), the National Natural Science Foundation of China (Grant No. 10872148), the National Hi-Tech Development Plan (863) (Grant No. 2008AA05Z413) and the Program for Young Excellent Talents in Tongji University (Grant No. 2010KJ065) are highly appreciated. Financial support from the China Scholarship Council for the second author's visiting the University of Southern California as a joint Ph.D. student is gratefully acknowledged. Prof. Roger Ghanem is greatly appreciated for his constructive discussions and comments on the researches.

## References

- Amini, F. and Tavassoli, M.R. (2005), "Optimal structural active control force, number and placement of controllers", *Eng. Struct.*, **27**, 1306-1316.

- Anderson, B.D.O. and Moore, J. (1990), *Optimal Control: Linear Quadratic Methods*, Prentice-Hall International Editions.
- Baber, T.T. and Wen, Y.K. (1981), "Random vibration of hysteretic degrading systems", *J. Eng. Mech. Div.*, **107**(6), 1069-1087.
- Baber, T.T. and Noori, M.N. (1985), "Random vibration of degrading, pinching systems", *J. Eng. Mech.*, **111**(8), 1010-1027.
- Bernstein, D.S. (1993), "Nonquadratic cost and nonlinear feedback control", *Int. J. Robust Nonlin.*, **3**, 211-229.
- Bouc, R. (1967), "Forced vibration of mechanical system with hysteresis", *Proceedings of the Fourth Conference on Nonlinear Oscillations*, Prague, Czechoslovakia.
- Chen, G.P., Malik, O.P., Qin, Y.H. and Xu, G.Y. (1992), "Optimization technique for the design of a linear optimal power system stabilizer", *IEEE T. Energy Convers.*, **7**(3), 453-459.
- Chen, J.B. and Li, J. (2005), "Dynamic response and reliability analysis of nonlinear stochastic structures", *Probabilist. Eng. Mech.*, **20**(1), 33-44.
- Chen, J.B. and Li, J. (2008), "Strategy for selecting representative points via tangent spheres in the probability density evolution method", *Int. J. Numer. Meth. Eng.*, **74**(13), 1988-2014.
- Chen, J.B., Liu, W.Q., Peng, Y.B. and Li, J. (2007), "Stochastic seismic response and reliability analysis of base-isolated structures", *J. Earthq. Eng.*, **11**(6), 903-924.
- Chung, J. and Lee, J.M. (1994), "A new family of explicit time integration methods for linear and nonlinear structural dynamics", *Int. J. Numer. Meth. Eng.*, **37**, 3961-3976.
- Clough, R.W. and Johnson, S.B. (1966), "Effects of stiffness degradation on earthquake ductility requirements", *Proceedings of the 2nd Japan National Earthquake Engineering Conference*, Tokyo, Japan.
- Clough, R.W. and Penzien, J. (1993), *Dynamics of Structures*, 2nd Edition, McGraw-Hill, New York.
- Eldred, M.S., Adams, B.M., Gay, D.M., Swiler, L.P., Haskell, K., Bohnhoff, W.J., Eddy, J.P., Hart, W.E., Watson, J.P., Griffin, J.D., Hough, P.D., Kolda, T.G., Williams, P.J. and Martinez-Canales, M.L. (2007), *DAKOTA, A Multilevel Parallel Object-Oriented Framework for Design Optimization, Parameter Estimation, Uncertainty Quantification, and Sensitivity Analysis* (Version 4.1+ User's Manual). Sandia National Laboratories, SAND 2006-6337.
- Foliente, G.C. (1995), "Hysteresis modeling of wood joints and structural systems", *J. Struct. Eng.*, **121**(6), 1013-1022.
- Iwan, W.D. (1961), *The Dynamics Response of Bilinear Hysteretic System*, California: California Institute of Technology.
- Li, J. and Ai, X.Q. (2006), "Study on random model of earthquake ground motion based on physical process", *Earthq. Eng. Eng. Vib.*, **26**(5), 21-26. (in Chinese)
- Li, J. and Chen, J.B. (2009), *Stochastic Dynamics of Structures*, John Wiley & Sons.
- Li, J., Peng, Y.B. and Chen, J.B. (2010a), "A physical approach to structural stochastic optimal controls", *Probabilist. Eng. Mech.*, **25**, 127-141.
- Li, J., Peng, Y.B. and Chen, J.B. (2010b), "Probabilistic criteria of structural stochastic optimal controls", *Probabilist. Eng. Mech.*, **26**(2), 240-253.
- Ma, F., Zhang, H., Bochstedte, A., Foliente, G.C. and Paevere, P. (2004), "Parameter analysis of the differential model of hysteresis", *J. Appl. Mech.*, **71**, 342-349.
- Masri, S.F., Bekey, G.A. and Caughey, T.K. (1981) "On-linear control of nonlinear flexible structures", *J. Appl. Mech.*, **49**, 871-884.
- Peng, Y.B., Ghanem, R. and Li, J. (2010), "Generalized optimal control policy for stochastic optimal control of structures", *Struct. Control Health Mon.* (revised and under review).
- Shefer, M. and Breakwell, J.V. (1987), "Estimation and control with cubic nonlinearities", *J. Optimiz. Theory App.*, **53**, 1-7.
- Suhardjo, J., Spencer, J.B.F. and Sain, M.K. (1992), "Nonlinear optimal control of a duffing system", *Int. J. Nonlin. Mech.*, **27**(2), 157-172.
- Wen, Y.K. (1976), "Method for random vibration of hysteretic systems", *J. Eng. Mech. Div.*, **102**(2), 249-263.
- Yang, J.N., Agrawal, A.K. and Chen, S. (1996), "Optimal polynomial control for seismically excited non-linear and hysteretic structures", *Earthq. Eng. Struct. D.*, **25**, 1211-1230.
- Yang, J.N., Akbarpour, A. and Ghaemmaghami, P. (1988), "Optimal control of nonlinear flexible structures",

- Technical Report NCEER-88-0002*, National Center for Earthquake Engineering Research.
- Yang, J.N., Li, Z., Danielians, A. and Liu, S.C. (1992), "Hybrid control of nonlinear and hysteretic systems I", *J. Eng. Mech.*, **118**(7), 1423-1440.
- Yang, J.N., Li, Z. and Vongchavalitkul, S. (1994), "Stochastic hybrid control of hysteretic structures", *Probabilist. Eng. Mech.*, **9**(1-2), 125-133.
- Yao, J.T.P. (1972), "Concept of structural control", *J. Struct. Div.*, **98**(7), 1567-1574.
- Zhu, W.Q., Ying, Z.G., Ni, Y.Q. and Ko, J.M. (2000), "Optimal nonlinear stochastic control of hysteretic systems", *J. Eng. Mech.*, **126**(10), 1027-1032.